Desalination and Water Treatment
www.deswater.com

doi: 10.5004/dwt.2017.20925

96 (2017) 86–96
November

Adsorption of sunset yellow by luffa sponge, modified luffa and activated carbon from luffa sponge

Fei Xu[a,†], Xiao-yu Qi[b,†], Qiang Kong[a,*], Li Shu[c], Ming-sheng Miao[d], Shiguo Xu[a], Yuan-da Du[a], Qian Wang[a], Qun Liu[d], Shuai-shuai Ma[d]

[a]*College of Geography and Environment, Shandong Normal University, 88 Wenhua Donglu, Jinan 250014, Shandong, China, Tel. +86 531 86182550; Fax: +86 531 86180107; emails: kongqiang0531@hotmail.com (Q. Kong), xufeisdnu@yahoo.com (F. Xu), mailxsg@126.com (S. Xu), 392331698@qq.com (Y. Du), qianwang86@sdnu.edu.cn (Q. Wang)*
[b]*No. 4 Middle School of Ningyang County, 118 Xinggang Road, Tai'an 271400, Shandong, China, email: 1737197806@qq.com*
[c]*School of Engineering, RMIT University, 402 Swanston Street, Melbourne, VIC 3000 Australia, email: li.shu846@gmail.com*
[d]*College of Life Science, Shandong Normal University, 88 Wenhua Donglu, Jinan 250014, Shandong, China, emails: mingshengmiao@163.com (M. Miao), 373400619@qq.com (Q. Liu), 2410191093@qq.com (S. Ma)*

Received 6 February 2017; Accepted 13 May 2017

ABSTRACT

We investigated the adsorption of sunset yellow (SY) in water by luffa sponge (LC)-based materials. Modified luffa sponge (MLC) and luffa sponge activated carbon (LAC) were prepared by chemical modification and H_3PO_4 activation, respectively, followed by charring. Dried LC adsorbs SY poorly through a physical adsorption process, with an equilibrium adsorption capacity of 14 mg/g at 298 K. MLC and LAC showed substantially improved adsorption of SY. The maximum equilibrium adsorption capacity of MLC for SY reached 137 mg/g – 9.78 times that of raw luffa – and this adsorbent had a maximum removal rate of 99.9%. The adsorption capacity of LAC for SY was even higher, with the maximum equilibrium adsorption rate reaching 476.19 mg/g and the maximum removal rate exceeding 99% at 298 K. The kinetics of absorption fit the pseudo-second-order kinetic equations for the three adsorbing agents, which suggests that the main limiting factor for adsorption is the adsorption mechanism. The isotherm curves for the three adsorbents fit the Langmuir isotherm equation with correlation coefficients above 0.99, which indicates the adsorption is monolayer adsorption.

Keywords: Luffa sponge; Modification; Activated carbon; Sunset yellow; Adsorption

1. Introduction

With the rapid growth of the Chinese economy and the improvement of people's livelihoods, there is increasing demand for water for industrial, agricultural and domestic use. Industrial wastewater is a leading source of environmental pollution, and dye wastewater is the most serious pollutant. Dyes are used in textiles, leather, papermaking, pharmaceuticals, food processing and industrial production [1,2], and the main types of dyes in current commodities are anionic, cationic and nonionic dyes. Dyes can produce a huge amount of sewage in production processes, with the discharge of dye wastewater accounting for around 35% of the gross discharge of industrial wastewater in China. This has become particularly important in recent years because of the booming textile industry [3]. An effective way to treat dye wastewater is thus urgently needed.

* Corresponding author.

† These authors contributed equally to this work.

Presented at the 9th International Conference on Challenges in Environmental Science & Engineering (CESE-2016), 6–10 November 2016, Kaohsiung, Taiwan.

Dye wastewater lowers the light permeability of water bodies, interfering with the photosynthesis of aquatic plants and retarding the growth of fauna and flora. Dyes can also jeopardise human health through biological accumulation in the food chain. Dye wastewater is complicated in composition, highly stable and not easily biodegradable. In addition, some dyes and their degradation products are highly toxic or very likely to cause deformation, cancer and mutation [3–5]. Sunset yellow (SY), an anionic dye mainly used for food and drug colouring, is one example. Consumption of large quantities or sustained consumption of foods containing SY can result in damage to the liver or kidneys [6,7].

Current treatments for dye wastewater can be divided into physicochemical and biological approaches. The most common treatments include adsorption, biological, chemical coagulation, chemical oxidation and electromechanical methods. Adsorption methods boast a series of advantages, for example, easy operation, extensive pH adaptability and no secondary pollution. For these reasons, adsorption methods are applied extensively with satisfactory effects [8–10]. Common adsorbents include ion-exchange fibres, industrial waste (e.g., coal ash and residue) and activated carbon. However, ion-exchange fibres are not applicable to nonionic dyes. Although coal ash and residue that have cellular structures are excellent adsorbents, their small specific surface areas make them less suitable for wastewater treatment [11–13].

Luffa is a crop mainly planted in temperate and subtropical areas, with large-scale cultivation across southern and northern China. Luffa has high value as a food source and for medical uses. Dried ripe luffa sponge (LC) is mainly composed of cellulose, hemicellulose and lignin. Cellulose and lignin are considered the best materials for the preparation of activated carbon. Ripe LC has large pores and a large specific surface area, which make it a natural adsorbent with good absorbency that can be modified or carbonised for the treatment of dye wastewater [14,15].

This study investigated the adsorption of SY by LC, modified luffa sponge (MLC) and luffa sponge activated carbon (LAC). The surface structures of the materials were analysed using scanning electron microscopy (SEM), and the structures of the surface functional groups were examined by infrared spectroscopy. The adsorption mechanisms were explored on the basis of pseudo-kinetic models, isothermal adsorption models and adsorption thermodynamics. This study contributes to the idea of using low-cost agricultural by-products, waste and activated carbon prepared from these materials for the purification of dye wastewater.

2. Materials and methods

2.1. Materials and chemicals

Luffa was obtained from a local market in Jinan Province, China. The seeds of dried LC were removed and crushed into particles with a grain diameter of 1–2 mm. Then, *N,N*-dimethylformamide and polyepichlorohydrin, each with a volume five times that of the seeds, ethanediamine with a volume four times that of the seeds, and triethylamine with a volume twice that of the seeds were sequentially poured into a beaker [16]. The ground LC seeds were added with a final ratio of 1:30 (mass of LC to volume of mixed liquid). The liquid mixture was placed in a standing-temperature cultivator at 80°C to allow chemical reaction for 7 h. The solids were collected and rinsed with deionised water until the filtrate was neutral. The solid was dried at 70°C for 12 h and cooled to room temperature to give the MLC adsorbent.

Clean LC was dried for 12 h at 100°C before being crushed into particles with an appropriate grain diameter using a grinder, and then dried for 12 h at 120°C for later use. The dried LC was soaked in 1:1 phosphoric acid solution for 12 h, with an LC mass to solution ratio of 1:5. This chemical activation was expected to increase the carbon yield and create a porous structure, and activation of the material with phosphoric acid may therefore have resulted in activated carbon with a high adsorption capacity [17]. The solids were dried for 1 h at 450°C, and then the cooled carbonised LC was rinsed with distilled water until the pH value was approximately 7. The rinsed material was dried for 12 h at 120°C and then cooled. Finally, the dried material was placed in a mortar for grinding and sieved to obtain LAC [18,19].

SY (CAS# 2783-94-0) was supplied by Sinopharm Chemical Reagent Co., Ltd., Shanghai, China, and used as received. SY has a molecular weight of 452.38 g/mol and a chemical formula of $C_6H_{10}N_2Na_2O_7S_2$. A stock solution (1,000 mg/L) of SY in distilled water was prepared and diluted as required. All other chemicals used were analytical grade. Distilled water was used throughout the experiment to prepare the solutions.

2.2. Physical characteristics of the adsorbent

The specific surface area and pore structure of LC, MLC and LAC were determined using a scanning electron microscope (SUPRA™ 55, Zeiss, Germany), a pore-size automatic analyser (Quadrasorb SI, Quantachrome, USA) with the N_2 static adsorption capacity method and a surface area analyser (Quantachrome), respectively. Samples were dried for 3 h at 0.133 Pa and 100°C. The adsorption–desorption isotherm line of N_2 was measured at 77 K. The total specific surface area was determined with the Brunauer–Emmett–Teller (BET) method. The pore-size distribution was obtained from density functional theory calculations. The total pore volume was calculated using the built-in software of the pore-size automatic analyser.

2.3. Adsorption equilibrium and removal rate

The adsorption characteristics of LC, MLC and LAC were tested using SY (λ_{max} = 482 nm). Solutions of different SY concentrations were prepared by diluting the stock solution with distilled water according to specific experimental demands. Absorbents were mixed with SY solution and filtered through a membrane after adsorption. The absorbency of the filtrate at 482 nm was measured using a spectrophotometer, and the concentration of SY dye in the solution was calculated based on a standard curve. The removal rate η and equilibrium adsorption capacity Q_e (mg/g) were calculated with Eqs. (1) and (2), respectively:

$$\eta(\%) = \frac{C_0 - C_e}{C_0} \times 100\% \quad (1)$$

$$Q_e = \frac{(C_0 - C_e)V}{W} \quad (2)$$

where C_0 and C_e represent the initial concentration of the dye and the concentration at adsorption equilibrium (mg/L), respectively; V represents the solution volume (L) and W represents the mass of the adsorbent (g).

2.4. Adsorption kinetics

The experimental adsorption data were fitted to pseudo-first-order, pseudo-second-order and intra-particle diffusion models.

The pseudo-first-order kinetic model is extensively used to describe adsorption kinetics in aqueous solution. The theoretical basis for the model is that the adsorption rate is influenced by solution concentration and adsorption capacity, and the limiting factor for adsorption is intra-particle mass transfer resistance. The pseudo-first-order kinetic model can be expressed as follows [20]:

$$\ln(Q_e - Q_t) = \ln Q_e - k_1 t \quad (3)$$

where Q_t is the adsorption quantity (mg/g) at time t and k_1 is the pseudo-first-order adsorption rate constant (1/min). The value of k_1 is obtained from the slope of the fitted straight line of a graph with t as the x-coordinate and $\ln(Q_e - Q_t)$ as the y-coordinate.

The pseudo-second-order kinetic equation is also widely used to describe adsorption kinetics. According to this model, the adsorption mechanism is the limiting factor, and intra-particle mass transfer does not limit the progress of adsorption. The expression for the pseudo-second-order kinetic equation is as follows [21]:

$$\frac{t}{Q_t} = \frac{1}{k_2 Q_e^{\,2}} + \frac{1}{Q_e} t \quad (4)$$

where $V_0 = k_2 Q_e^{\,2}$.

In Eq. (4), V_0 represents the initial adsorption rate of the adsorption process (mg/g min) and k_2 represents the pseudo-second-order adsorption rate constant (g/mg min). The values of Q_e, k_2 and V_0 can be obtained from the slope and intercept of the fitted straight line of a graph with t as the x-coordinate and t/Q_t as the y-coordinate.

The particle diffusion equation describes adsorbate transfer from the solution to the solid surface as occurring mainly through intra-particle diffusion, which controls the adsorption rate in a variety of adsorption processes. The existence of these control processes can be achieved using the intra-particle diffusion equation [22]:

$$Q_t = k_p t^{1/2} + C \quad (5)$$

where k_p represents the rate constant for the intra-particle diffusion equation (mg/g min$^{1/2}$) and C represents the intercept, which reflects the thickness of the boundary layer. Smaller values of C correspond to a smaller effect of the boundary layer on the adsorption. The values of k_p and C can be obtained from the slope and intercept of the fitted straight line of a graph with $t^{1/2}$ as the x-coordinate and Q_t as the y-coordinate. A straight line passing through the origin ($C = 0$) shows that the only factor controlling the adsorption rate is the intra-particle diffusion process.

2.5. Adsorption isotherms

The Langmuir adsorption isotherm equation is mainly used to describe monolayer adsorption, with the general expression (Eq. (6)) and linear form (Eq. (7)) as follows [23]:

$$Q_e = \frac{Q_m K_L C_e}{1 + K_L C_e} \quad (6)$$

$$\frac{C_e}{Q_e} = \frac{1}{Q_m K_L} + \frac{1}{Q_m} C_e \quad (7)$$

where K_L represents the Langmuir constant (L/mg), which reflects the adsorption rate and Q_m represents the maximum adsorption capacity of the adsorbent (mg/g). Q_m and K_L values are obtained from the slope and intercept, respectively, of the fitted straight line of a graph with C_e as the x-coordinate and C_e/Q_e as the y-coordinate.

The Freundlich isotherm equation is based on a theory of multi-layer molecular adsorption, and assumes that there are multiple correlations between adsorbate and adsorbent. The general expression (Eq. (8)) and linear expression (Eq. (9)) for the Freundlich isotherm equation are as follows [24]:

$$Q_e = K_F C_e^{\frac{1}{n}} \quad (8)$$

$$\ln Q_e = \ln K_F + \frac{1}{n} \ln C_e \quad (9)$$

where K_F is the Freundlich constant (mg/g) with $1/n$, which represents the adsorption capacity and n represents the adsorption intensity. Larger values of n indicate better adsorption performances. The value of n is obtained from the slope of the fitted straight line, and that of K_L is obtained from the intercept of the fitted straight line of a line graph with $\ln C_e$ as the x-coordinate and $\ln Q_e$ as the y-coordinate.

Eq. (10) gives the Dubinin–Radushkevich (D–R) equation [25]:

$$\ln Q_e = \ln Q_m - \beta\varepsilon^2 \qquad \varepsilon = RT\ln\left(1 + \frac{1}{Ce}\right) \quad (10)$$

where $E = (2\beta) -1/2$.

In Eq. (10), R represents the ideal gas constant (8.314 J/mol K); β represents the adsorption energy constant (kJ^2/mol^2); T represents the thermodynamic temperature (K), ε represents the Polanyi potential and E represents the average adsorption free energy (kJ/mol). The values of Q_m and β

are obtained from the intercept and slope, respectively, of the fitted straight line of a graph with $\ln Q_e$ as the y-coordinate and ε^2 as the x-coordinate, and the value of E can be calculated according to Eq. (10).

2.6. Adsorption thermodynamics

The thermodynamic state function of adsorption involves the following parameters: enthalpy change (ΔH, kJ/mol), entropy change (ΔS, J/mol K) and free energy change (ΔG, kJ/mol), and these can be calculated with Eqs. (11) and (12) [26].

$$\Delta G = -RT\ln K \tag{11}$$

$$\ln K = \frac{\Delta S}{R} - \frac{\Delta H}{RT} \tag{12}$$

The value of K can be obtained from the isotherm model calculation. ΔH is obtained from the slope and ΔS from the intercept of the fitted straight line of a graph with $1/T$ as the x-coordinate and $\ln K$ as the y-coordinate.

3. Results and discussion

3.1. Analysis of adsorbent characteristics

LC has many irregular structures on its surface, as shown in the SEM images before and after modification (Figs. 1(a) and (b), respectively), which give LC a high specific surface area and good adsorption capacity. Substantial chemical changes, which are consistent with chemical modification, take place on the surface of modified LC and change its structure (Fig. 1(b)). The surface of LAC is uneven, with large gaps and some pore structures (Fig. 1(c)), which greatly increase the specific surface area [27]. The BET specific surface area of LC before and after modification was 10.12 and 5.19 m^2/g, respectively. Although modification lowered the specific surface area of MLC, the maximum equilibrium adsorption capacity of SY increased substantially. This suggests that the enhanced adsorption capacity is because of chemical factors, which indicates that the adsorption process is chemical adsorption and best simulated by the D–R equation [28]. The specific surface area of activated carbon increased to 834 m^2/g, 82 times that of LC, which suggests that the drastic increase in the specific surface area is a major contributing factor to the great improvement in the adsorption capacity for SY.

The pore-size distribution curve for activated carbon can be obtained from the nitrogen adsorption–desorption isotherm. Fig. 2 shows the pore-size distribution of LAC. The pores of activated carbon are mainly 1.0–2.0 nm micropores and 2.0–50 nm mesopores. The specific surface area of the activated carbon was calculated as 834 m^2/g, of which 31.2% and 68.8% are present as micropores and mesopores, respectively, indicating that LAC has a typical mixed micropore–mesopore structure. Micropores play a key role in accelerating the adsorption process through capillary condensation, which enhances the adsorption performance of activated carbon to a total pore capacity of as high as 1.012 cm^3/g [29]. This structure gives LAC distinct adsorption advantages.

The infrared spectra of LC, MLC and LAC are shown in Fig. 3. The bands at 2,920 and 1,460 cm^{-1} correspond to the stretching vibration of $–CH_3$, with considerable changes taking place on both sides of the two wave bands for MLC and LAC [16]. The 3,429 cm^{-1} band corresponds to the stretching vibration of –OH. The 1,738 and 1,650 cm^{-1} absorptions

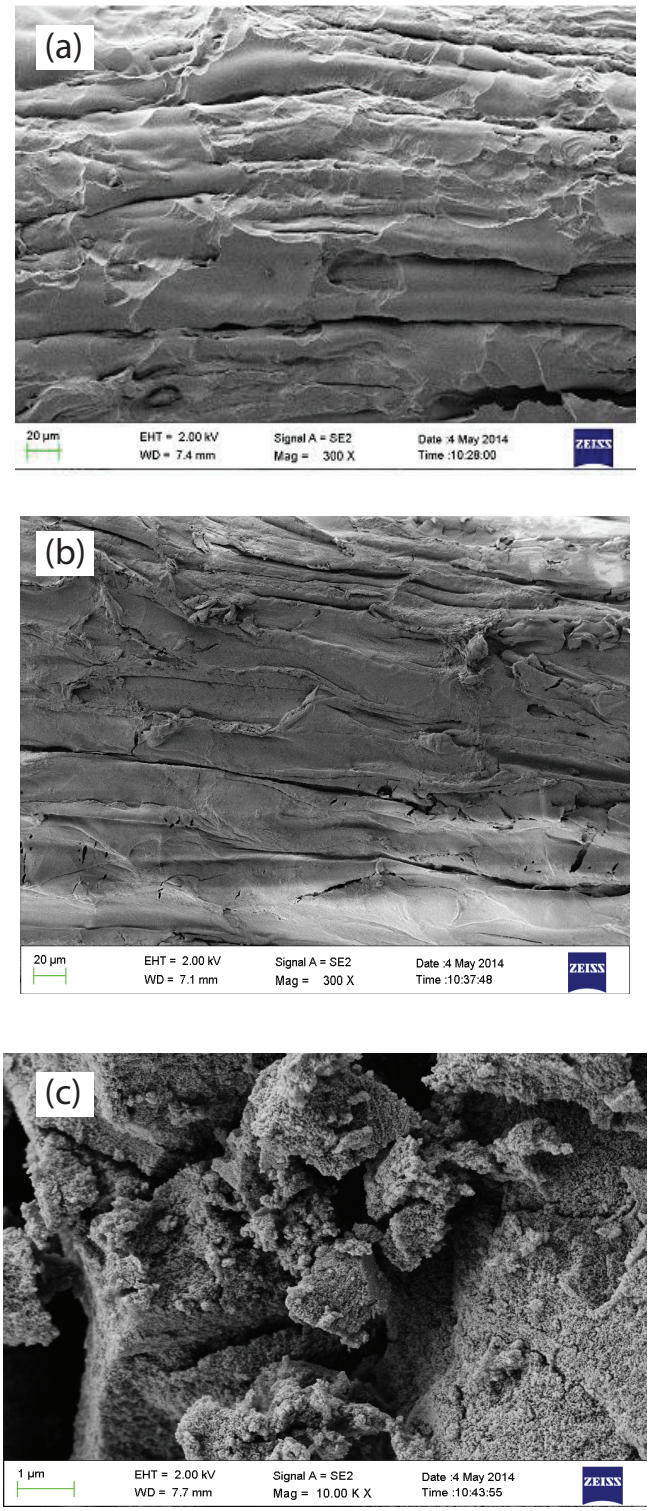

Fig. 1. Surface figure of (a) LC, (b) MLC and (c) LAC.

correspond to the stretching vibration of aldehyde groups and the C=O in amides. The 1,057 and 1,253 cm^{-1} peaks correspond to ether bonds, and show great changes after modification. There may thus be an increase in the number of ether bonds after modification [14]. The 558 cm^{-1} band corresponds to the –CH functional group in *o*-xylene, which does not show any considerable changes after modification [30]. The above results show that the notable enhancement of the adsorption capacity of MLC for SY may be the result of changes in the functional groups, particularly in the methyl and ether bonds [31]. These functional groups thus appear to play a key role in the adsorption of SY.

3.2. Effect of adsorbent dosage

The influence of the dosage of LC on the equilibrium adsorption capacity and removal rate of SY is shown in Fig. 4(a). The removal rate rises continuously with increasing adsorbent dosage, but the equilibrium adsorption capacity remains almost unchanged. This phenomenon can be explained as follows: more dye is adsorbed as the number of adsorption sites increases with increasing LC dosage, which leads to the rise in the removal rate; however, the equilibrium adsorption capacity remains unchanged despite the increased LC dosage when the adsorption reaches saturation [32]. A 2.0 g/L dose was chosen as optimal after considering the cost of the adsorbent and the rate of removal, and this dose was used for all further experiments.

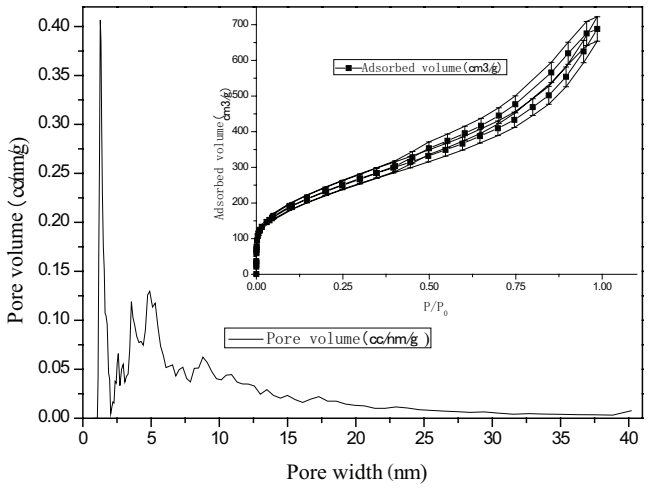

Fig. 2. Pore-size distribution and N_2 adsorption–desorption isotherms (inset) obtained for LAC.

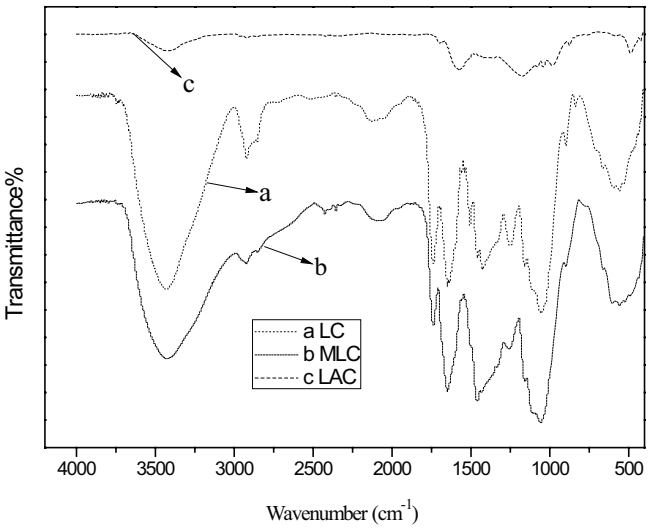

Fig. 3. FTIR spectra of LC, MLC and LAC.

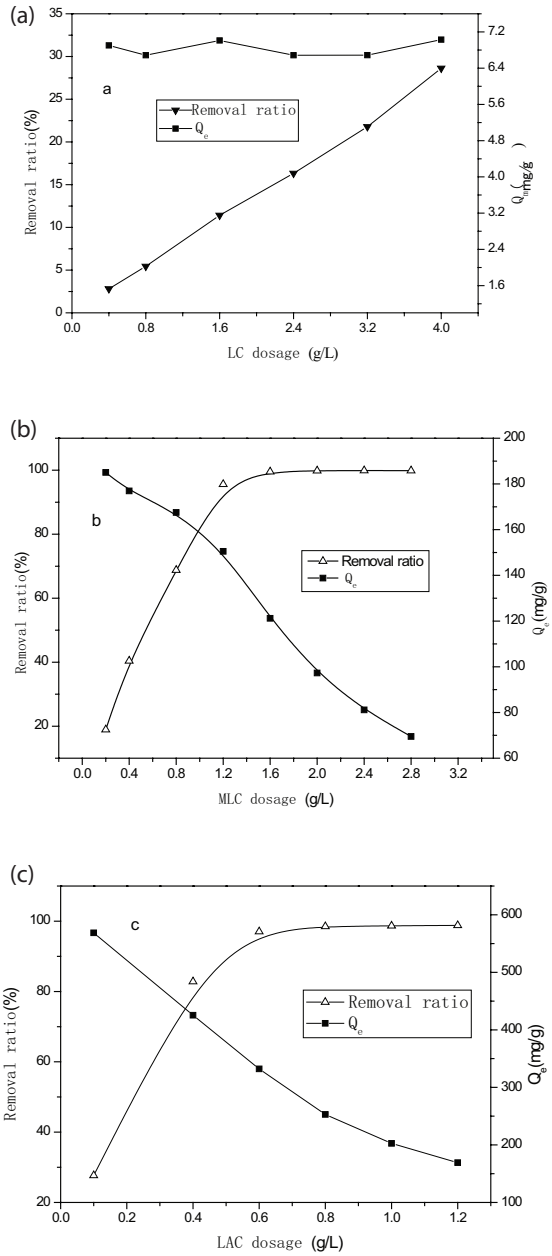

Fig. 4. Effect of adsorbent dosage on SY removal rates and equilibrium adsorption amount: (a) LC (pH = 1, C_0 = 100 mg/L, t = 180 min, T = 25°C ± 1°C); (b) MLC (C_0 = 200 mg/L, t = 180 min, T = 25°C ± 1°C) and (c) LAC (pH = 1, C_0 = 200 mg/L, t = 180 min, T = 25°C ± 1°C).

The influence of MLC dosage on the equilibrium adsorption capacity for SY is shown in Fig. 4(b). The removal rate increased with the adsorbent dosage, while the equilibrium adsorption capacity steadily decreased. The mechanism underlying this phenomenon is similar to that for LAC discussed below. The optimal dosage of this absorbent based on the removal rate and equilibrium adsorption capacity was 1.2 g/L.

The influence of the LAC dosage on the equilibrium adsorption capacity for SY is shown in Fig. 4(c). The SY removal rate shows an initial rapid increase with increasing LAC dosage, and the increase gradually becomes slower. The cause of the increased removal rate with increasing LAC dosage can be ascribed to saturation of the adsorbent surface at low dosages, which corresponds to a fast initial removal rate [33]. The removal rate remains relatively stable as the removal approaches 100%. The equilibrium adsorption capacity gradually decreases at higher dosages of LAC, which indicates that two factors (removal rate and equilibrium adsorption capacity) should be taken into account. Based on the above factors, the optimal dosage of activated carbon was 0.8 g/L. At the beginning of the adsorption, there were many available surface sites. The changes in the removal rate and adsorption capacity with increasing dosage were a result of saturation of the available surface sites. Repulsive forces between the solvated SY molecules resulted in no obvious differences between the adsorption capacities of SY on MLC and on LAC [34].

3.3. Effect of pH on absorption

The influence of pH on the adsorption capacity of LC for SY is shown in Fig. 5. The error in each data point was determined by multiple measurements and is relatively small. The removal rate and equilibrium adsorption capacity of SY by LC were greatly influenced by pH, with adsorption becoming more effective at low pH (Fig. 5(a)); this thus indicates that the optimal pH value is 1. The percentage removal decreased as the pH increased; this is attributed to SY adsorption occurring through electrostatic interactions or hydrogen bonding with the various functional groups of the adsorbent [35,36]. The influence of pH on the adsorption capacity of MLC for SY is shown in Fig. 5(b). The pH had little impact on the equilibrium adsorption capacity and removal rate, and the pH was therefore left unadjusted for subsequent experiments using MLC. In contrast, the pH had a notable influence on the removal rate and equilibrium adsorption capacity of LAC for SY (Fig. 5(c)), with better adsorption in strongly acidic conditions. This may be because the number of positively charged sites increases with increasing acidic strength, and these sites favour the adsorption of anionic SY molecules because of electrostatic attraction to the LAC surface [32,37]. The pH value was adjusted to 1 for subsequent experiments with LAC.

3.4. Effect of contact time and adsorption kinetics

The influence of the adsorption time on the removal rate of SY by LC, MLC and LAC is shown in Figs. 6(a)–(c), respectively. The removal rate of SY increases continuously with increasing adsorption time, and reaches equilibrium after 180 min. The adsorption rate was rapid for the first 90 min because of the presence of numerous vacant adsorption sites at the early stages of the process. The uptake became almost constant after agitating for 180 min for all concentrations; this could be because of the limited number of vacant sites and repulsive forces among the solvated molecules [38].

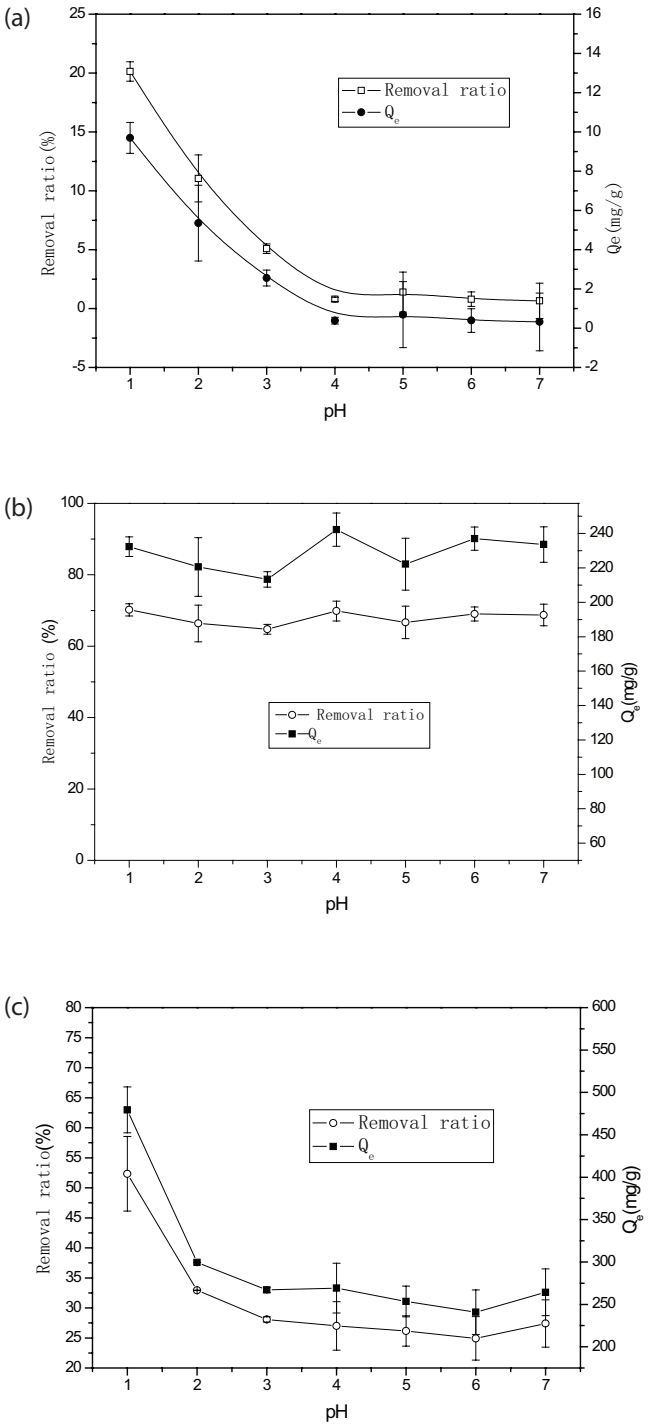

Fig. 5. Solution pH effects on SY adsorption: (a) LC (sorbent dose = 2 g/L, C_0 = 100 mg/L, t = 180 min, T = 25°C ± 1°C); (b) MLC (sorbent dose = 1.2 g/L, C_0 = 400 mg/L, t = 180 min, T = 25°C ± 1°C) and (c) LAC (sorbent dose = 0.2 g/L, C_0 = 200 mg/L, t = 180 min, T = 25°C ± 1°C).

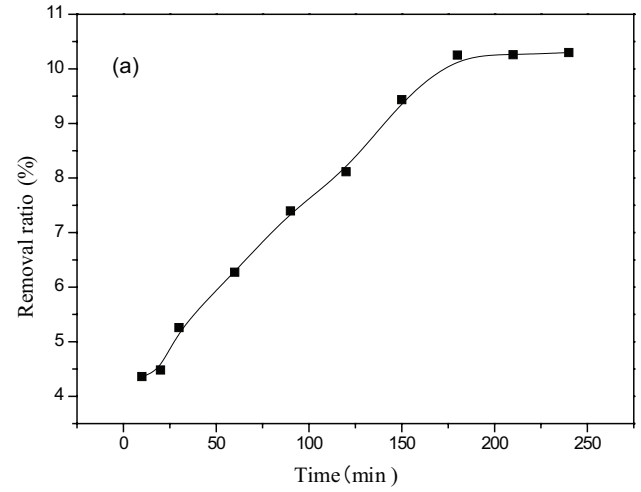

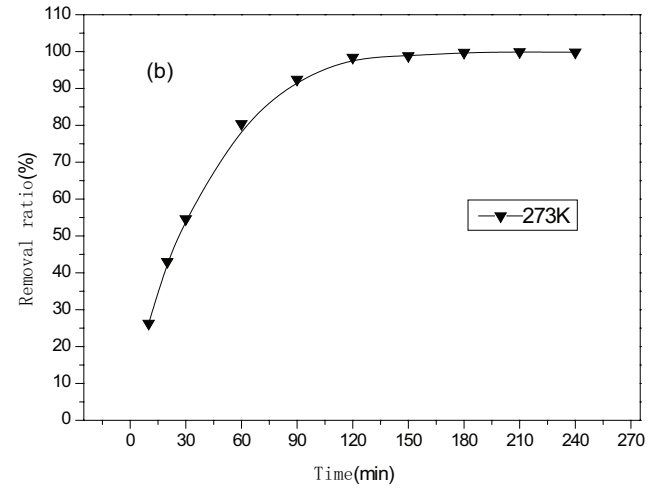

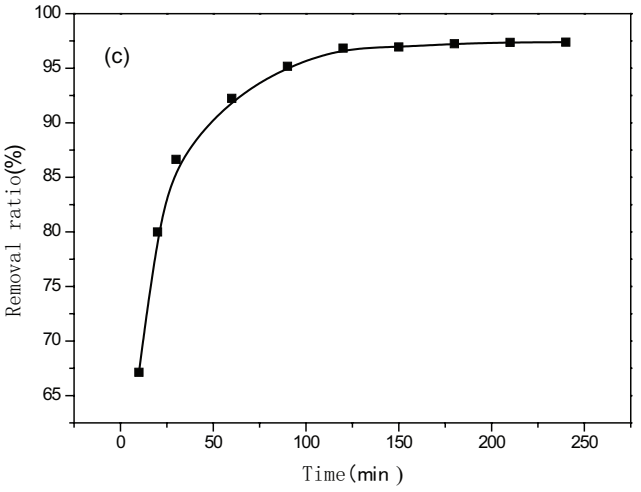

Fig. 6. Effect of adsorption time on SY removal: (a) LC (sorbent dose = 0.2 g/L, C_0 = 100 mg/L, pH = 1, T = 25°C ± 1°C); (b) MLC (sorbent dose = 1.2 g/L, C_0 = 200 mg/L, pH = 1, T = 25°C ± 1°C) and (c) LAC (sorbent dose = 0.8 g/L, pH = 1, C_0 = 200 mg/L, T = 25°C ± 1°C).

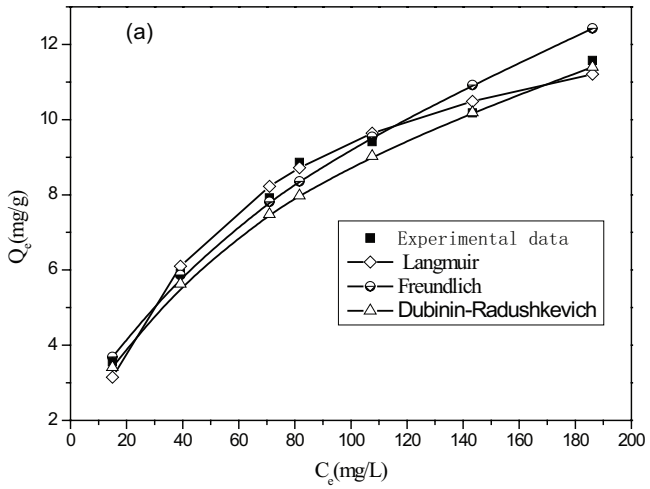

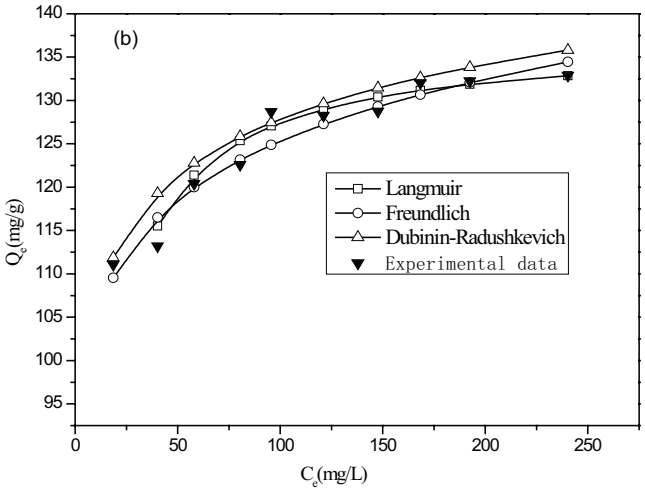

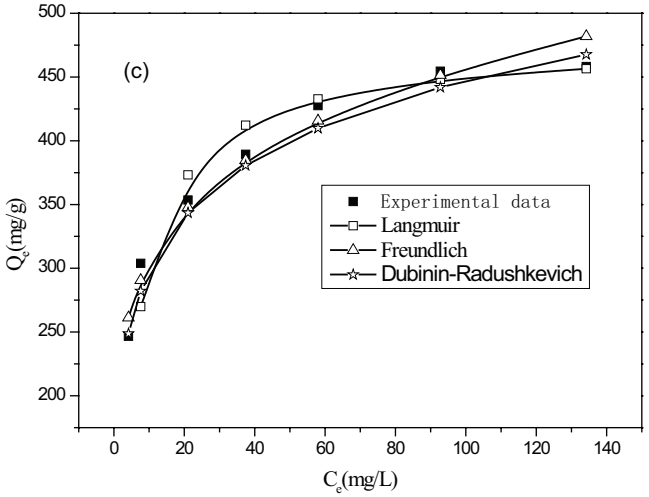

Fig. 7. Experimental and fitted data from the Langmuir, Freundlich and D–R isotherm equations for adsorption of SY: (a) LC (sorbent dose = 2 g/L, pH = 1, t = 180 min, T = 25°C ± 1°C); (b) MLC (sorbent dose = 1.2 g/L, t = 180 min, T = 25°C ± 1°C) and (c) LAC (sorbent dose = 0.8 g/L, pH = 1, t = 180 min, T = 25°C ± 1°C).

An equilibrium adsorption time of 180 min was used for all further experiments with the three adsorbents. Table 1 shows the kinetic fit results for the adsorption of SY by LC, MLC and LAC. Based on the correlation coefficients, the equilibrium adsorption capacity of all three adsorbents is best described by the pseudo-second-order kinetic model. This suggests that the adsorption mechanism, not intra-particle mass transfer resistance, is the limiting factor for the adsorption capacity of the three adsorbents. The kinetic simulation results for adsorption of SY by MLC at various temperatures are shown in Table 2. The equilibrium adsorption capacity of MLC for SY increased continuously with increasing temperature. This agrees with the conclusions drawn from the isotherm curve simulation, in which the maximum adsorption capacity increased with temperature, and those from the thermodynamic simulation, which suggested that SY adsorption is an endothermic process [39,40].

3.5. Effect of initial concentration and adsorption isotherms

Various initial SY concentrations were selected to investigate the influence of adsorbate concentration on the adsorption process and to simulate the adsorption isotherm curve. The solutions were oscillated until adsorption equilibrium was reached, and the absorbency was determined after filtration. The equilibrium concentration and equilibrium adsorption capacity were calculated and simulated using the Langmuir, Freundlich and D–R isotherm equations. The relationships between the equilibrium concentrations of SY after adsorption and LC, MLC and LAC are shown in Figs. 7(a)–(c), respectively. The equilibrium adsorption capacity is closest to the theoretical values obtained from the Langmuir simulation at 298 K (Table 3). Thus, it can be concluded that SY is adsorbed by monolayer adsorption [39].

The simulated isotherm curve model of MLC is shown in Table 3. The maximum adsorption capacity is directly proportional to temperature, and that of MLC peaks at a temperature of 298 K with a maximum of 137 mg/g, which is 9.78 times that of LC (14 mg/g). The reported maximum equilibrium adsorption capacities of other adsorbents for SY are much lower, e.g., kohlrabi peel (26.32 mg/g) and peanut shell (13.99 mg/g) [41,42]. Moreover, MLC can effectively remove SY from water, with the removal rate exceeding 99%. The average adsorption free energy is $E > 20$ kJ/mol, which indicates that this is chemical adsorption. Table 4 shows the adsorption results of the three adsorbents and the relevant parameters for the Langmuir, D–R and Freundlich isotherm curve fitting. LAC was the best of the three adsorbents for adsorption of SY, with a maximum adsorption capacity as high as 476 mg/g.

3.6. Factors affecting the results of the orthogonal experiment

Orthogonal experimental design and analysis is the most commonly used method for experimental optimisation.

Table 1
Parameters of pseudo-first-order, pseudo-second-order and particle diffusion kinetic models for adsorption of SY by LC at 298 K

Adsorbent	Experimental date Q_e (mg/g)	Pseudo-first-order			Pseudo-second-order				Particle diffusion		
		k_1 (min^{-1})	Q_e (mg/g)	R^2	k_2 (g/mg min)	Q_e (mg/g)	V_0 (mg/g min)	R^2	k_p (mg/g $min^{1/2}$)	C (mg/g)	R^2
LC	9.90	0.0252	13.60	0.837	2.31×10^{-3}	11.36	0.30	0.9779	0.5287	2.20	0.9794
MLC	166	0.0268	140	0.9921	2.64×10^{-4}	181	8.74	0.9991	9.60	39.57	0.8696
LAC	277.30	0.0328	104.4	0.9817	7.8×10^{-4}	285	63.69	0.9999	5.72	202.8	0.7483

Table 2
Parameters of pseudo-first-order, pseudo-second-order and particle diffusion kinetic models for adsorption of SY by MLC at various temperatures

Temperature (K)	Experimental date Q_e (mg/g)	Pseudo-first-order			Pseudo-second-order				Particle diffusion		
		k_1 (min^{-1})	Q_e (mg/g)	R^2	k_2 (g/mg min)	Q_e (mg/g)	V_0 (mg/g min)	R^2	k_p (mg/g $min^{1/2}$)	C (mg/g)	R^2
288	123	0.0259	121	0.9327	3.71×10^{-4}	133	6.59	0.9950	6.79	33.12	0.9343
298	166	0.0268	140	0.9921	2.64×10^{-4}	181	8.74	0.9991	9.60	39.57	0.8696
308	167	0.0357	222	0.9868	1.79×10^{-4}	192	6.63	0.9954	9.84	36.99	0.8543

Table 3
Fitted Langmuir, Freundlich and D–R isotherm parameters for adsorption of SY by MLC at various temperatures

Temperature (K)	Langmuir			Freundlich			Dubinin–Radushkevich			
	Q_m (mg/g)	K_L (L/mg)	R^2	$1/n$	K_F $(mg/g)^{1/n}$	R^2	β (mol^2/J^2)	Q_m (mg/g)	E (kJ/mol)	R^2
288	109	0.1646	0.9977	0.0514	81	0.4805	6.0×10^{-10}	127	28.87	0.6476
298	137	0.1339	0.9993	0.0801	87	0.9300	7.0×10^{-10}	173	26.73	0.9261
308	192	0.5591	0.9969	0.0603	142	0.9470	8.0×10^{-10}	226	25.00	0.9509

An orthogonal experiment can be designed based on the actual level and number of factors that affect the experimental results [43]. Tables 5–7 show the results of orthogonal experiments on the adsorption of SY by LC, MLC and LAC. A three-factor, three-level, nine-group experiment was selected for MLC because pH has little impact on its adsorption of SY and was therefore not considered an influential factor for this adsorbent. In contrast, pH had a considerable effect on the adsorption of SY by LC and LAC, and a four-factor, three-level, nine-group experiment was selected for these adsorbents. The optimal adsorption by LC, MLC and LAC was found by weighing the factors of removal rate and equilibrium adsorption capacity. The optimal pH value, temperature, adsorbent dosage and initial concentration of SY were, respectively, 1, 318 K, 2.4 mg/L and 250 mg/L for LC; 318 K, 0.8 mg/L, 200 mg/L for MLC (pH was not considered for this adsorbent); and 1, 313 K, 0.8 mg/L, 250 mg/L for LAC. The removal rate and equilibrium adsorption capacity reached 14.68% and 15.28 mg/g; 97.39% and 243.47 mg/g; and 98.54% and 253.01 mg/g for LC, MLC and LAC, respectively.

3.7. Effect of the three adsorbents on the equilibrium adsorption capacity and removal rate of SY

Fig. 8 shows the removal rates and equilibrium adsorption capacities of SY by LC, MLC and LAC at 298 K.

Table 4
Fitted Langmuir, Freundlich and D–R isotherm parameters for adsorption of SY by various adsorbents at 298 K

Adsorbent	Langmuir equation			Freundlich equation			Dubinin–Radushkevich equation			
	Q_m (mg/g)	K_L (L/mg)	R^2	$1/n$	K_F (mg/g)$^{1/n}$	R^2	β (mol^2/J^2)	Q_m (mg/g)	E (kJ/mol)	R^2
LC	14	0.0187	0.9902	0.4814	1.00	0.9875	4.0×10^{-9}	56.7	11.18	0.9935
MLC	137	0.1339	0.9993	0.0801	87	0.9300	7.0×10^{-10}	173	26.73	0.9261
LAC	476	0.1721	0.9987	0.176	203	0.9714	1.5×10^{-9}	859	22.36	0.9821

Table 5
Orthogonal experiment results for adsorption of SY by LC

Level	Experiment condition and result					
	pH	Temperature (K)	LC dosage (mg/L)	Concentration C_0 (mg/L)	Removal ratio η (%)	Adsorption capacity Q_e (mg/g)
1	1	308	1.6	150	10.18	9.48
2	1	313	2.0	200	14.05	14.43
3	1	318	2.4	250	14.68	15.28
4	2	318	1.6	200	13.85	18.63
5	2	308	2.0	250	10.05	12.55
6	2	313	2.4	150	8.93	5.43
7	3	313	1.6	250	2.89	4.65
8	3	318	2.0	150	9.46	7.58
9	3	308	2.4	200	5.87	4.85

Table 6
Orthogonal experiment results for adsorption of SY by MLC

Level	Experiment condition and result				
	Temperature (K)	MLC dosage (mg/L)	Concentration C_0 (mg/L)	Removal ratio η (%)	Adsorption capacity Q_e (mg/g)
1	318	0.8	200	97.39	243.47
2	318	1.2	150	99.94	125.09
3	318	1.6	250	99.93	155.30
4	313	0.8	250	76.50	240.18
5	313	1.2	200	99.64	166.99
6	313	1.6	150	99.96	94.63
7	308	0.8	150	92.40	174.94
8	308	1.2	250	83.47	173.47
9	308	1.6	200	99.94	125.47

Table 7
Orthogonal experiment results for adsorption of SY by LAC

Level	Experiment condition and result					
	pH	Temperature (K)	LAC dosage (mg/L)	Concentration C_0 (mg/L)	Removal ratio η (%)	Adsorption capacity Q_e (mg/g)
1	1	308	0.6	150	97.53	242.30
2	2	308	0.8	200	87.40	275.01
3	3	308	1.0	250	90.99	180.41
4	1	313	0.8	250	98.54	253.01
5	2	313	1.0	150	97.22	141.89
6	3	313	0.6	200	67.51	289.77
7	1	318	0.6	250	84.48	351.74
8	2	318	1.0	200	97.31	209.45
9	3	318	0.8	150	91.47	183.07

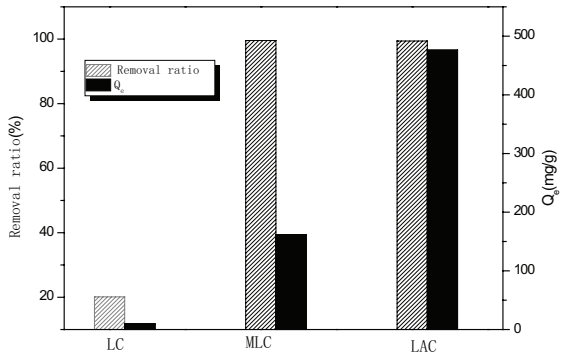

Fig. 8. SY removal efficiency and equilibrium adsorption amount at 298 K for LC, MLC and LAC.

The removal rate reached 20.13%, 99.55% and 99.41% for LC, MLC and LAC, respectively, with equilibrium adsorption capacities of 9.70, 161.29 and 476.19 mg/g, respectively. The maximum adsorption capacity of MLC and LAC is 15.6 and 48 times that of LC, respectively, which suggests that the adsorption capacity of luffa increases considerably after modification or carbonisation. LAC shows the best adsorption of SY in terms of removal rate and equilibrium adsorption capacity.

4. Conclusion

The methyl and ether functional groups on the surface of luffa-based absorbents play an important role in the adsorption of SY, giving MLC considerably better absorption characteristics than LC. The BET specific surface area of LC before modification was 10.12 m^2/g; this decreased to 5.19 m^2/g for MLC and increased to as much as 834 m^2/g for LAC. The specific surface area of LAC is composed of 31.2% micropores and 68.8% mesopores, and this adsorbent has a typical mixed micropore–mesopore structure. The total pore volume of LAC is as high as 1.012 cm^3/g. Adsorption by LC is physical adsorption. After chemical modification, the surface of LC is positively charged, which greatly enhances its capacity for the adsorption of anionic dyes to 9.78 times that before modification. The adsorption of SY by MLC is thus a chemical adsorption process. The Langmuir isotherm equation gives the best simulation results for the isothermal adsorption process of the three adsorbents, with correlation coefficients all above 0.99. This indicates that the adsorption process is a monolayer adsorption. The maximum adsorption capacity of MLC for SY is directly proportional to the temperature, which means that the adsorption is an active endothermic process. The kinetics of adsorption for the three adsorbents are best simulated by the pseudo-second-order kinetic equation, which suggests that the main limiting factor for adsorption is the adsorption mechanism. MLC could be used extensively in the treatment of SY containing wastewater because it efficiently adsorbs high levels of SY. Optimal adsorption of SY was achieved at a pH value, temperature, adsorbent dosage and initial concentration of SY of, respectively, 1, 318 K, 2.4 mg/L and 250 mg/L (LC); 318 K, 0.8 mg/L and 200 mg/L (MLC, no pH value was determined for this adsorbent); and 1, 313 K, 0.8 mg/L and 250 mg/L (LAC). The removal rates and equilibrium adsorption capacities of LC, MLC and LAC reached 14.68% and 15.28 mg/g, 97.39% and 243.47 mg/g, and 98.54% and 253.01 mg/g, respectively. The removal rates of SY by LC, MLC and LAC reached 20.13%, 99.55% and 99.41%, respectively, with corresponding equilibrium adsorption capacities of 9.70, 161.29 and 476.19 mg/g. LAC was the best adsorbent for SY among the three adsorbents tested.

Acknowledgements

This work was supported by the Promotional research fund for excellent young and middle-aged scientists of Shandong Province (No. BS2014HZ019 and No. ZR2016CB18), the China Postdoctoral Science Foundation (No. 2014M551950), A Project of Shandong Province Higher Educational Science and Technology Program (No. J15LE07), National Natural Science Foundation of China (No. 51608315) and the Major Science and Technology Program for Water Pollution Control and Treatment (No. 2012ZX07203004, 2015ZX07203005 and 2015ZX07203-007-005).

References

[1] E.P. Chagas, L.R. Durrant, Decolorization of azo dyes by *Phanerochaete chrysosporium* and *Pleurotus sajorcaju*, Enzyme Microb. Technol., 29 (2001) 473–477.

[2] P.K. Malik, Use of activated carbons prepared from sawdust and rice-husk for adsorption of acid dyes: a case study of Acid Yellow 36, Dyes Pigm., 56 (2003) 239–249.
[3] D. Shen, J. Fan, W. Zhou, B. Gao, Q. Yue, Q. Kang, Adsorption kinetics and isotherm of anionic dyes onto organo-bentonite from single and multisolute systems, J. Hazard. Mater., 172 (2009) 99–107.
[4] K. Kadirvelu, M. Kavipriya, C. Karthika, M. Radhika, N. Vennilamani, S. Pattabhi, Utilization of various agricultural wastes for activated carbon preparation and application for the removal of dyes and metal ions from aqueous solutions, Bioresour. Technol., 87 (2003) 129–132.
[5] H. Wu, J. Fan, Z. Jian, H.H. Ngo, W. Guo, L. Shuang, J. Lv, S. Lu, W. Wu, S. Wu, Intensified organics and nitrogen removal in the intermittent-aerated constructed wetland using a novel sludge-ceramsite as substrate, Bioresour. Technol., 210 (2016) 101–107.
[6] T.M. Coelho, E.C. Vidotti, M.C. Rollemberg, A.N. Medina, M.L. Baesso, N. Cella, A.C. Bento, Photoacoustic spectroscopy as a tool for determination of food dyes: comparison with first derivative spectrophotometry, Talanta, 81 (2010) 202–207.
[7] H. Wu, Z. Jian, H.H. Ngo, W. Guo, H. Zhen, L. Shuang, J. Fan, L. Hai, A review on the sustainability of constructed wetlands for wastewater treatment: design and operation, Bioresour. Technol., 175 (2014) 594–601.
[8] F.P.D. Sá, B.N. Cunha, L.M. Nunes, Effect of pH on the adsorption of Sunset Yellow FCF food dye into a layered double hydroxide (CaAl-LDH-NO_3), Chem. Eng. J., 215–216 (2013) 122–127.
[9] S.E. Bailey, T.J. Olin, R.M. Bricka, D.D. Adrian, A review of potentially low-cost sorbents for heavy metals, Water Res., 33 (1999) 2469–2479.
[10] H. Wu, J. Fan, Z. Jian, H.H. Ngo, W. Guo, H. Zhen, L. Shuang, Decentralized domestic wastewater treatment using intermittently aerated vertical flow constructed wetlands: impact of influent strengths, Bioresour. Technol., 176 (2014) 163–168.
[11] A.K. Jain, V.K. Gupta, A. Bhatnagar, Suhas, Utilization of industrial waste products as adsorbents for the removal of dyes, J. Hazard. Mater., 101 (2003) 31–42.
[12] C.D. Woolard, J. Strong, C.R. Erasmus, Evaluation of the use of modified coal ash as a potential sorbent for organic waste streams, Appl. Geochem., 17 (2002) 1159–1164.
[13] S. Wang, M. Soudi, L. Li, Z.H. Zhu, Coal ash conversion into effective adsorbents for removal of heavy metals and dyes from wastewater, J. Hazard Mater., 133 (2006) 243–251.
[14] A. Altınışık, E. Gür, Y. Seki, A natural sorbent, *Luffa cylindrica* for the removal of a model basic dye, J. Hazard. Mater., 179 (2010) 658–664.
[15] H. Demir, A. Top, D. Balköse, S. Ülkü, Dye adsorption behavior of *Luffa cylindrica* fibers, J. Hazard. Mater., 153 (2008) 389–394.
[16] V.O.A. Tanobe, T.H.D. Sydenstricker, M. Munaro, S.C. Amico, A comprehensive characterization of chemically treated Brazilian sponge-gourds (*Luffa cylindrica*), Polym. Test., 24 (2005) 474–482.
[17] Q.S. Liu, Z. Tong, W. Peng, G. Liang, Preparation and characterization of activated carbon from bamboo by microwave-induced phosphoric acid activation, Ind. Crop Prod., 31 (2010) 233–238.
[18] M. Miao, Y. Wang, Q. Kong, L. Shu, Adsorption kinetics and optimum conditions for Cr(VI) removal by activated carbon prepared from luffa sponge, Desal. Wat. Treat., 57 (2016) 7763–7772.
[19] J. Li, Z. Ren, Y. Ren, L. Zhao, S. Wang, J. Yu, Activated carbon with micrometer-scale channels prepared from luffa sponge fibers and their application for supercapacitors, RSC Adv., 4 (2014) 35789–35796.
[20] W.J. Weber, J.C. Morris, Kinetics of adsorption on carbon from solution, J. Sanitary Eng. Div. Proc. Am. Soc. Civil Eng., 1 (1963) 1–2.
[21] Y.S. Ho, G. Mckay, Pseudo-second order model for sorption processes, Process Biochem., 34 (1999) 451–465.
[22] C. Yao, T. Chi, Approximate solution of intraparticle diffusion equations and their application to continuous-flow stirred tank and fixed-bed adsorption calculations, Sep. Technol., 4 (1994) 67–80.
[23] Y. Liu, Some consideration on the Langmuir isotherm equation, Colloids Surf., A, 274 (2006) 34–36.
[24] B. Xiang, L.I. Yi-Jiu, Applications of isothermal adsorption equations to heavy metal ions adsorption phenomena, Nonferrous Met., 59 (2007) 77–80.
[25] B. Mcenaney, Estimation of the dimensions of micropores in active carbons using the Dubinin-Radushkevich equation, Carbon, 25 (1987) 69–75.
[26] Y.H. Li, Z. Di, J. Ding, D. Wu, Z. Luan, Y. Zhu, Adsorption thermodynamic, kinetic and desorption studies of Pb^{2+} on carbon nanotubes, Water Res., 39 (2005) 605–609.
[27] S. Li, M. Tao, Y. Xie, Reduced graphene oxide modified luffa sponge as a biocomposite adsorbent for effective removal of cationic dyes from aqueous solution, Desal. Wat. Treat., 57 (2016) 20049–20057.
[28] I.O. Mazali, O.L. Alves, Morphosynthesis: high fidelity inorganic replica of the fibrous network of loofa sponge (*Luffa cylindrica*), An. Acad. Bras. Ciênc., 77 (2005) 25–31.
[29] Y.K. Liu, M. Seki, S. Furusaki, Plant cell immobilization in loofa sponge using two-way bubble circular system, J. Chem. Eng. Jpn., 32 (1999) 8–14.
[30] M. Wang, J. Zhang, Y. Gao, X. Yang, J. Zhao, Determination of Sunset Yellow in soft drinks at attapulgite modified expanded graphite paste electrode, J. Electrochem Soc., 161 (2013) H86–H91.
[31] Y.Z. Sun, X.P. Zhang, R.M. Gong, H.J. Liu, Y. Chao, Effect of chemical modification on dye adsorption capacity of peanut hull, Dyes Pigm., 67 (2006) 175–181.
[32] M. Ghaedi, A.H. Jah, Cadmium telluride nanoparticles loaded on activated carbon as adsorbent for removal of sunset yellow, Spectrochim. Acta, Part A, 90 (2012) 22–27.
[33] M.A.M. Salleh, D.K. Mahmoud, A.W.A.K. Wan, A. Idris, Cationic and anionic dye adsorption by agricultural solid wastes: a comprehensive review, Desalination, 280 (2011) 1–13.
[34] Q. Kong, Y. Wang, L. Shu, M. Miao, Isotherm, kinetic, and thermodynamic equations for cefalexin removal from liquids using activated carbon synthesized from loofah sponge, Desal. Wat. Treat., 57 (2016) 7933–7942.
[35] J.F. Osma, V. Saravia, J.L. Toca-Herrera, S.R. Couto, Sunflower seed shells: a novel and effective low-cost adsorbent for the removal of the diazo dye Reactive Black 5 from aqueous solutions, J. Hazard. Mater., 147 (2007) 900–905.
[36] Q. Kong, Q. Liu, M. Miao, Y. Liu, Q. Chen, C. Zhao, Kinetic and equilibrium studies of the biosorption of sunset yellow dye by alligator weed activated carbon, Desal. Wat. Treat., 66 (2017) 281–290.
[37] Y. Wang, Q. Liu, L. Shu, M. Miao, Y. Liu, Q. Kong, Removal of Cr(VI) from aqueous solution using Fe-modified activated carbon prepared from luffa sponge: kinetic, thermodynamic, and isotherm studies, Desal. Wat. Treat., 57 (2016) 29467–29478.
[38] M. Ghaedi, A. Hekmati Jah, S. Khodadoust, R. Sahraei, A. Daneshfar, A. Mihandoost, M.K. Purkait, Cadmium telluride nanoparticles loaded on activated carbon as adsorbent for removal of sunset yellow, Spectrochim. Acta, Part A, 90 (2012) 22–27.
[39] M. Ghaedi, Comparison of cadmium hydroxide nanowires and silver nanoparticles loaded on activated carbon as new adsorbents for efficient removal of Sunset yellow: kinetics and equilibrium study, Spectrochim. Acta, Part A, 94 (2012) 346–351.
[40] Z. Qi, Q. Liu, Z.R. Zhu, Q. Kong, Q.F. Chen, C.S. Zhao, Y.Z. Liu, M.S. Miao, C. Wang, Rhodamine B removal from aqueous solutions using loofah sponge and activated carbon prepared from loofah sponge, Desal. Wat. Treat., 57 (2016) 29421–29433.
[41] R. Gong, X. Zhang, H. Liu, Y. Sun, B. Liu, Uptake of cationic dyes from aqueous solution by biosorption onto granular kohlrabi peel, Bioresour. Technol., 98 (2007) 1319–1323.
[42] H. Nadi, M. Alizadeh, M. Ahmadabadi, A.R. Yari, S. Hashemi, Removal of reactive dyes (green, orange, and yellow) from aqueous solutions by peanut shell powder as a natural adsorbent, Arch. Hyg. Sci. 1 (2012) 41–47.
[43] W.F. Dong, L.H. Zang, Q.L. Feng, Orthogonal experiments for optimizing adsorption of methyl orange from aqueous solution, Adv. Mater. Res., 726–731 (2013) 2241–2245.